

Low-Carbon Economic Multi-Objective Dispatch of an Integrated Energy System Based on GAPSO

Minglei Qin^{1,*}, Anjie Lu², Yu Huang³

¹*School of Electrical Engineering, Southeast University, Nanjing, China*

²*School of Government, Nanjing University, Nanjing, China*

³*Institute of Advanced Technology for Carbon Neutrality, Nanjing University of Posts and Telecommunications, Nanjing, China*

**qml0815@163.com, city_pro@163.com, huangyu@njupt.edu.cn*

Abstract—In recent years, several countries have proposed targets for carbon neutrality in energy, and the transformation of energy systems has become a research hotspot. As a system capable of coupling multi-energy, achieving high penetrations of renewable energy, and improving energy efficiency, the integrated energy system will take on more responsibility under the carbon neutrality target. This paper uses GAPSO (which combines genetic algorithm with particle swarm optimisation algorithm, has a faster iteration speed, and avoids local optimisation) to solve the Pareto frontier set considering the system operation costs and carbon emission. The system operation costs are described using Latin hypercube sampling (LHS) to predict the stochastic output of the renewable energy source and a penalty function based on the predicted mean vote (PMV) model to describe the thermal comfort of the user, which is solved using the genetic algorithm (GA) algorithm. The carbon emission is calculated using the carbon accounting method.

Index Terms—Low-carbon integrated energy systems; Carbon emission accounting; Multi-objective optimisation; GAPSO.

I. INTRODUCTION

Recently, carbon neutrality has been the focus of much research in the energy industry. China has pledged to take strong measures to achieve a carbon peak by 2030 and carbon neutrality by 2060. Meanwhile, the U.S. and the European Union have proposed to achieve carbon neutrality by 2050 [1]. In electricity, buildings, transportation, and fossil fuels, the electricity industry has the highest carbon emissions and is the key to achieving carbon neutrality [2]. In existing research on the low-carbon transformation of the electricity industry, high penetrations of renewable energy [3], the use of low-carbon and clean energy technologies, including energy storage equipment [4], multi-energy coupling equipment [5], renewable energy generation [6], gas-fired power plants, and electric hydrogen production equipment, are particularly critical. In contrast, the integrated energy

system (IES) can achieve coordinated planning and flexible dispatch of multiple energy systems, effectively improve energy use efficiency, promote the consumption of renewable energy generation, and reduce operating costs which prove to be an essential vehicle for the low-carbon transformation process.

The integrated energy system was first proposed in [7], and has been widely studied, taking advantage of energy coupling [8], multi-energy complementarity [9], and improving storage conversion flexibility. The heat pump, boiler, combined heat, and power plant are introduced in [10] to realise the couple of electric, thermal, natural gas, and other forms of energy, which have been widely used at the district level, regional level, and park level. The utility of the integrated energy system can effectively reduce operating costs and increase the accommodation of renewable energy [11], [12]. In early studies of IES optimisation, the minimum operating cost of the system and the maximum user profitability were usually taken as objectives, focussing only on the economy of the system, and the optimisation process was relatively homogeneous. In later studies, using a two-level optimisation algorithm, the lower-level objectives, such as user thermal comfort [12], energy storage equipment cost [13], and secondary user profitability [14], are combined to form a two-level model while ensuring upper-level objectives, resulting in more comprehensive results and greater significance of the reference for realistic operation. Alternatively, a multi-objective optimisation model can be built from multiple aspects such as energy cost, energy efficiency level [15], and demand response [16], using Pareto optimal or heuristic algorithms to achieve optimisation under multi-objective considerations. In general, previous studies have done less research on optimising the low-carbon characteristics of integrated energy systems, which do not meet the requirements for the low-carbon attributes of integrated energy systems in the context of carbon neutrality.

In this paper, we develop a low-carbon economic multi-objective dispatch of an integrated energy system considering carbon emission accounting. The main

contributions of this work are summarised as follows:

1. The Latin hypercube sampling (LHS) and a penalty function based on the predicted mean vote (PMV) model have been presented to model the stochastic output of renewable energy and thermal comfort, respectively, and the genetic algorithm (GA) has been used to solve for the convex quadratic functions of the operating costs;
2. The carbon accounting method and the ladder penalty mechanism have been introduced to define the carbon trading costs for carbon emissions;
3. The GAPSO algorithm, which combines the GA with the particle swarm algorithm, has a faster iteration speed and avoids local optimisation, and has been used to solve the Pareto frontier set considering the system operation costs and carbon emissions.

II. FRAMEWORK OF THE INTEGRATED ENERGY SYSTEM

The proposed integrated energy system is shown in Fig. 1. In terms of electricity supply, it primarily meets the electricity demand of customers through the upper grid, various distributed energy sources, and combined heat and power (CHP) units, where distributed energy sources include photovoltaic, wind energy, and battery energy storage system. In terms of gas consumption, natural gas is transmitted directly from the upper gas grid to customers' homes or CHP units through gas pipelines, and the additional gas tank is added during the transmission process to avoid blockages caused by excessive air pressure and transmission rate during the gas transmission process, affecting gas consumption of customers. The customer's heat needs are met by an electric boiler in conjunction with the CHP unit.

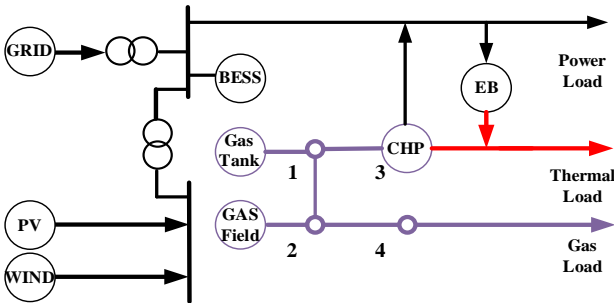


Fig. 1. Structure of the IES network.

In the process of building equipment models, various converters and storages are integrated for combining and coupling these carriers to form redundant connections within the hub-internal energy and can offer a certain degree of flexibility and synergies for multi-energy supplies, as shown in (1)

$$\begin{bmatrix} L_E \\ L_H \\ L_G \end{bmatrix} = \begin{bmatrix} C_{11} & C_{12} & C_{13} \\ C_{21} & C_{22} & C_{23} \\ C_{31} & C_{32} & C_{33} \end{bmatrix} \times \begin{bmatrix} S_E \\ S_H \\ S_G \end{bmatrix}, \quad (1)$$

where L_E , L_H , and L_G are the electricity load, thermal load, and gas load, respectively. S_E , S_H , and S_G are the energy of electricity, heat, and gas, respectively.

The elements of the matrix on the left (1) denote electricity, thermal, and gas, the dispatch factor of each energy-use device, converter device, and energy storage.

III. MULTI-OBJECTIVE OPTIMISATION MODEL

A. Minimum Integrated Operating Costs

1. Latin hypercube sampling

LHS is a random sampling method to solve the uncertainty of renewable energy output. Compared to the Monte Carlo method, it has the average allocation of sampling probability and can take into account the role of the interaction between different sampling functions [17]. The basic LHS equation is shown in (2)

$$r_{m,l} = F_{Z_m}^{-1}\left(\frac{l-a}{L}\right), \quad m=1,2,\dots,M, \quad l=1,2,\dots,L, \quad (2)$$

where $r_{m,l}$ is the sampling value in the m^{th} variable's l^{th} section; $F_{Z_m}^{-1}$ is the corresponding inverse function of the cumulative distribution function (CDF).

However, the LHS method is unstable with the sample size. Therefore, this paper uses the modified LHS method as a random sampling function of the new energy output [18]. The nearest matrix is found by the improved alternating projection method, and we modify the nearest matrix to guarantee its symmetry and positive character. The alternating projection method is as shown in (3), (4), in which the output X is the expected correlation matrix represented by P in (5):

$$P_{\text{rand}} = \begin{bmatrix} 1 & \rho_{r_{12}} & \dots & \rho_{r_{1N}} \\ \rho_{r_{21}} & 1 & \dots & \rho_{r_{2N}} \\ \vdots & \vdots & \ddots & \vdots \\ \rho_{r_{N1}} & \rho_{r_{N2}} & \dots & 1 \end{bmatrix}, \quad (3)$$

$$\begin{aligned} \rho_{r_{ij}} &= \rho(r_i, r_j) = \\ &= \frac{\text{cov}(r_i, r_j)}{\sigma_{r_i} \sigma_{r_j}} = \\ &= \frac{\text{cov}(r_j, r_i)}{\sigma_{r_j} \sigma_{r_i}} = \rho_{r_{ji}}, \end{aligned} \quad (4)$$

where r_i and r_j are the sampling values, σ_{r_i} and σ_{r_j} are the standard deviations of r_i and r_j , and $\text{cov}(r_j, r_i)$ is the covariance of r_i and r_j ,

$$\begin{aligned} X &= P_U(P_S(P_U(\dots P_S(P)))) \rightarrow P, \\ P_U(P) &= P - \text{diag}(\text{diag}(P - I)), \\ P_S(P) &= Z \times \text{diag}(\max(v_i, 0)) \times Z^T, \\ P &= ZAZ^T, \\ A &= \text{diag}(v_i). \end{aligned} \quad (5)$$

2. Thermal comfort of customers

This paper considers the response of the user's energy demand by building the PMV model in (6) [19]. According to China ISO7730, the user temperature is maintained at [23.5 °C–28.5°C]

$$D_{PMV} = \begin{cases} 0.9895(T - 26), & T \geq 26, \\ 0.4065(-T + 26), & T < 26. \end{cases} \quad (6)$$

Therefore, the thermal load demand of users per unit of

time can be changed to meet the thermal load demand of the thermal comfort range of users. Using consideration to meet the thermal load demand of the comfort range of users, reduce the overall thermal load pressure in central winter heating and decrease the overall energy consumption in the region to achieve the carbon emissions [12], as follows

$$\text{Min} \sum_{t \in T} [\text{price}_e^t \times (P_B^t + P_{CHP,e}^t) + \sigma \times (T_{in}^{t+1} - T_{opt})^2], \quad (7)$$

where σ is the penalty factor and can be determined from [12], T_{in}^{t+1} is the indoor temperature at the $(t + 1)^{th}$ time slot, and T_{opt} is the temperature most comfortable according to PMV.

3. Minimum cost objective function

For the integrated energy system proposed in this paper, its total operating costs can be expressed by the following equation, which contains six parts

$$\text{min } F_1 = \sum_{t=1}^T [F_{u,t} + F_{re,t} + F_{chp,t} + F_{lo,t} + F_{con,t} + F_{\sigma,t}] \times \Delta t, \quad (8)$$

where $F_{u,t}$ is the cost of purchasing electricity and gas energy, $F_{re,t}$ is the penalty cost of wind or photovoltaic abandonment, $F_{chp,t}$ is the operating cost of the CHP unit, $F_{lo,t}$ is the cost of energy charging and discharging loss, $F_{con,t}$ is the operation and maintenance costs of the equipment, and $F_{\sigma,t}$ is the equation of the penalty function considering thermal comfort of the user, visible (7).

$$F_{u,t} = \sum_{t=1}^T [\text{price}_e^t \times P_{grid,t} + \text{price}_{gas}^t \times V_{grid,t}] \times \Delta t, \quad (9)$$

where price_e^t is the price of electricity in the t^{th} period, price_{gas}^t is the price of gas in the t^{th} period, $P_{grid,t}$ is the electricity purchased from the upper grid in the t^{th} period, and $V_{grid,t}$ is the quantity of gas purchased from the upper network in the t^{th} period.

$$F_{re,t} = \sum_{t=1}^T [\lambda_w \times (P_{w,t}^f - P_{w,t}^{act}) + \lambda_p \times (P_{pv,t}^f - P_{pv,t}^{act})] \times \Delta t, \quad (10)$$

where λ_w is the unit penalty for abandoning wind power, $P_{w,t}^f$ is the forecast power of the wind generators in the t^{th} time slot, $P_{w,t}^{act}$ is the actual power used by the wind generators in the t^{th} time slot, λ_p is the unit penalty for abandoning photovoltaic power, $P_{pv,t}^f$ is the forecast power of the photovoltaic devices in the t^{th} time slot, and $P_{pv,t}^{act}$ is the power used of the photovoltaic devices in the t^{th} time slot.

$$F_{chp,t} = \sum_{t=1}^T [\lambda_{on}^{CHP} \times u_t \times (1 - u_{t-1}) + \lambda_{off}^{CHP} \times u_{t-1} \times (1 - u_t)] \times \Delta t, \quad (11)$$

where λ_{on}^{CHP} and λ_{off}^{CHP} are the start-up/shut-down cost of the CHP unit and u_t is the binary variable, 1 or 0, to represent on or off state of CHP in the t^{th} time slot.

$$F_{lo,t} = \sum_{t=1}^T \lambda_{loss} \times [P_{ch,t} \times (1 - \eta_e^{ch}) + P_{dis,t} \times (1 - \eta_e^{dis})] \times \Delta t + \sum_{t=1}^T \lambda_{loss} \times [V_{ch,t} \times (1 - \eta_{tank}^{ch}) + V_{dis,t} \times (1 - \eta_{tank}^{dis})] \times \Delta t, \quad (12)$$

where λ_{loss} is the cost of energy loss, $P_{ch,t}$ is the charging power of the battery energy system in the t^{th} time slot, $P_{dis,t}$ is the discharging power of the battery energy system in the t^{th} time slot, η_e^{ch} is the charging efficiency of the battery energy system, and η_e^{dis} is the discharging efficiency of the battery energy system.

$$F_{con,t} = \sum_{t=1}^T [\alpha_{chp} \times P_{chp,t} + \alpha_{eb} \times P_{eb,t} + \alpha_{pv} \times P_{pv,t}^f + \alpha_{wind} \times P_{w,t}^f + \alpha_{BESS} \times (P_{ch,t} + P_{dis,t}) + \alpha_{tank} \times (V_{ch,t} + V_{dis,t})] \times \Delta t, \quad (13)$$

where α_{chp} is the maintenance charge of the CHP unit, α_{eb} is the maintenance charge of the electric boiler, α_{wind} is the maintenance charge of the wind power unit; α_{BESS} is the maintenance charge of the battery energy system, α_{tank} is the maintenance charge of the gas tank, and α_{pv} is the maintenance charge of the photovoltaic power unit.

B. Minimum Carbon Emissions

By reducing the actual carbon emissions minus the free carbon emissions obtained by the energy purchase, the carbon emissions generated by the actual operation of each piece of equipment in this system are obtained

$$\text{min } F_2 = \sum_{t=1}^T C_{em} \times \Delta t, \quad (14)$$

where F_2 is the carbon emissions and C_{em} is the number of actual carbon emissions

$$C_{em} = E_{co_2} - E_{co_2}^*, \quad (15)$$

here E_{co_2} is the number of total carbon emissions and $E_{co_2}^*$ is the number of free carbon emissions.

The carbon emission measurement model can be known from (14), which can include the total carbon emission and voluntary compensation carbon emission. Usually, the total carbon emission minus the voluntary compensation carbon emission can obtain the real carbon emission of the system. The specific calculation equation, due to the limited space of the article, can be seen in the literature [20].

C. Network Constraint

In addition to the multi-objective functions, the typical constraints of the proposed IES can be divided into six parts: multi-energy balance constraints in (1); equipment output and input constraints [16]; battery constraints [13]; natural gas storage constraints [12]; CHP unit constraints [21]; constraints of the natural gas pipeline in [12]. A non-linear quadratic model appears in the constraints of the CHP unit

and the constraints of natural gas pipelines, and piecewise linear functions have been used to ensure the determined size and the specific method [22].

IV. SOLUTION METHOD

Based on the multi-objective model built in the previous chapter, this chapter first uses the genetic algorithm, which considers the quadratic form of the objective function, then uses the multi-objective solution method based on GAPSO to discuss the Pareto frontier sets.

Due to the limited length of the article, the standard genetic algorithm is not interpreted in the article, which can be seen in the literature [23]. The standard particle swarm optimisation (PSO) algorithm is known from the literature [24], the particle update strategy in the algorithm can be seen in (16), (17):

$$V_i(t+1) = \omega V_i(t) + c_1 r_1 (P_{besti} - X_i(t)) + c_2 r_2 (Z_{best} - X_i(t)), \quad (16)$$

$$X_i(t+1) = X_i(t) + V_i(t+1), \quad (17)$$

where $i = 1, 2, 3, \dots, m$, ω is the weight of inertia and c_1, c_2 are constants, indicating the approach to the own optimal and the global optimal; c_1 is called the “own factor”, c_2 is called the “global factor”, which is a random number, located in $[0, 1]$.

According to (16) and (17), the particles in the population are periodically updated and the optimal solution to the problem is gradually obtained. This paper intends to combine the genetic algorithm with the improved PSO algorithm to solve the model, and it can include the following two parts.

1. Inertial weight

According to (16) and (17), the velocity of the particle is greatly affected by the inertial weight; when it is large, the search ability is strong to search the unexplored area, the exploration ability weak, focus on the search for the solved attachment area, and the local search ability is strong. If the inertial weight can be adjusted according to the environmental information of the population and timely fed back to the next group iteration, then this will undoubtedly be highly applicable. To this end, this paper makes an adaptive adjustment of the inertia weight based on the dispersion of the group. The strategy is as follows.

– Step 1: When the PSO iterates, get the two particles with the largest distance $X_i(t) X_j(t)$, and get the direction vector of the two particles $\alpha(t)$.

– Step 2: The projection of all particles on the direction vector $\alpha(t)$ constitutes a set $f(t)$

$$f(t) = \alpha(t)^T \times x(t). \quad (18)$$

– Step 3: Divide $\alpha(t)$ according to the population size and count the number of particles projected in each interval $g_i(t)$.

– Step 4: Obtain the population dispersion at each iteration $E(t)$ according to (16) and (17):

$$E(t) = -\sum_{i=1}^n h_i(t) \times \ln h_i(t), \quad (19)$$

$$h_i(t) = \frac{g_i(t)}{n}. \quad (20)$$

– Step 5: Get the inertial weight of each generation

$$w(t) = \frac{1}{1 + 1.5e^{-2.6E(t)}}. \quad (21)$$

2. Introduce the elite ageing mechanism and the replacement mechanism.

Although PSO has the characteristics of fast convergence speed, it can be seen from the update equation of the particle swarm algorithm that the Z_{best} (optimal particle) is the update orientation in the whole optimisation process. Once the local optimal falls at a later stage, the whole particle population will also appear as a “precocious” phenomenon and the optimal solution cannot be obtained. For this reason, this paper considers introducing the elite ageing mechanism and the turnover mechanism into the PSO to weaken the guiding ability of the local optimal particles and avoid falling into the local optimum.

The adaptive real-time adjustment of *age* of the optimal individual particle is based on the guiding ability of the optimal individual in the iterative optimisation process. The update strategy is as follows:

$$age = \begin{cases} age + 2, & \delta_{Z_{best}} < 0, \\ age + 1, & \delta_{Z_{best}} = 0 \ \& \ \sum_{i=1}^n \delta_{Z_{best} < 0}, \\ age, & \delta_{Z_{best}} = 0 \ \& \ \sum_{i=1}^n \delta_{Z_{best} = 0}, \end{cases} \quad (22)$$

$$\delta_{Z_{best}}(t) = F(Z_{best}(t)) - F(Z_{best}(t-1)), \quad (23)$$

$$\sum_{i=1}^n \delta_{P_{best}}(t) = \sum_{i=1}^n F(P_{best}(t)) - \sum_{i=1}^n F(P_{best}(t-1)). \quad (24)$$

Equation (22) indicates the degree of optimisation of the global optimal value of the particle population and (23) indicates the degree of optimisation of the individual extreme joint optimisation of the particle population. For the minimum optimisation problem, the more negative the guiding ability, the stronger, while the guiding ability is weak, and it is easy to fall into the local optimum.

The above polynomial variation strategy [25], using the cloned individual as the parent e , following the following equation to obtain the parent g

$$g_j = e_j + (x_j^u - x_j^l) \delta_j, \quad (25)$$

where g_j, e_j represents the j^{th} component of g, e, x_j^u, x_j^l represent the maximum minimum of the j^{th} component of the variable to optimise, and δ_j calculates the following equation:

$$\delta_j = (2r_j)^{\frac{1}{\gamma+1}} - 1, 0 \leq r_j \leq 0.5, \quad (26)$$

$$\delta_j = 1 - [2(1-r_j)]^{\frac{1}{\gamma+1}}, 0.5 \leq r_j \leq 1, \quad (27)$$

where r_j is the random number distributed in $[0, 1]$; the degree of variation γ is the variation factor.

V. CASE STUDIES

A. Basic Configurations

The system architecture underpinning the scenario discussed in the manuscript is illustrated in Fig. 1. This diagram depicts the configuration encompassing a power grid integrated with a 1200 kWh battery energy storage system, photovoltaic apparatus, and a wind turbine.

In terms of gas use, the network contains four nodes that join the upper gas field, gas tank, CHP unit, and residents. Meanwhile, the thermal load can be satisfied by an electric boiler or a CHP unit whose installed capacity is 800 kW and 3300 kW. The parameters of all other units, the electric load, the gas load of a typical winter day for the next 24 hours, and the predicted temperature with electricity price are given in [26]. The basic gas price is 2.73 m³/¥, the fluctuation of the price is based on the model proposed in Chapter II, and the parameters of the natural gas networks are detailed in [12]. This case is implemented in MATLAB R2020b and Gurobi (Version 9.1.2), a commercial optimisation solver.

B. Analysis of Multi-Objective Optimisation

From Table I, it can be seen more intuitively that in minimum carbon emissions (MEC), the operating costs of the system will increase, mainly: in terms of energy purchase, the purchase from the upper grid, and gas network will be increased, and the dependence on external energy sources

TABLE I. OPERATING COSTS OF MOC AND MEC.

Modes	Operating costs (¥)	Maintenance costs (¥)	Energy flow costs (¥)	Energy purchasing costs (¥)	Thermal comfort costs (¥)
MOC	42113	3796.1	2466.9	34168	527.3
MEC	45925	3832.6	2779.7	37537	569.6

TABLE II. CARBON EMISSIONS OF MOC AND MEC.

Modes	Total carbon emissions (kg)	Actual carbon emissions (kg)	Free carbon emissions (kg)	Actual power carbon emissions (kg)	Actual gas carbon emissions (kg)
MOC	15642	44754	29112	16089	28664
MEC	13990	39938	25948	13506	26432

C. Penalty Factors

In this paper, Fig. 2 shows the user heating demands, as well as the heating method under various operating strategies. It can be found that under different strategies, the electric boiler does not always work during the 3 p.m.–8 p.m. period, and the analysis shows that the user's heating demand is low during this period and the electricity price is at a high level, so the CHP unit is used in preference for heating. The analysis shows that CHP units are preferred in the MEC mode as a result of their thermoelectric coupling. At night, when the electricity price is at a low level, the electric boiler is preferred, both for economic reasons and for carbon emission reasons. Therefore, when using small integrated energy systems for heating, electric boilers should be considered more often at night when the electricity price is low and CHP units during the day when the electricity price is high.

Figure 3 shows the effect of different penalty factors on internal room temperature. In comparison with Fig. 2 above, it can be found that the penalty factor is set up to a certain extent in line with the objective of carbon emission; with a low penalty factor, the internal room temperature is lower, the room heat supply is smaller, and the carbon emission of

will be greater; in terms of renewable energy sources, due to the increased dependence on external energy sources, the consumption of renewable energy sources will be reduced to a certain extent, and the amount of wind and photovoltaic abandoned by renewable energy sources will be expanded; in terms of energy transmission, electrical energy storage and the gas tank will be used more frequently; in terms of heating, the penalty cost for judging the thermal comfort of users will become greater, while the carbon emissions of the system will be reduced, the thermal comfort of the system will be reduced.

Table II shows the carbon emissions of the system in minimum operating costs (MOC) and MEC, respectively. In the context of carbon emissions, the impact of the MEC is evident. The system results in a notable decrease in electricity procurement from the upper tier. Moreover, the thermoelectric coupling of the combined heat and power (CHP) unit within the MEC serves to address the deficit in customer electrical load arising from the diminished electricity procurement. Furthermore, this coupling efficiently mitigates the decreased heat supply stemming from the reduced output of the electric boiler, thus ensuring swift compensation. Therefore, it can be seen that the economics of direct terminal purchase of electricity is greater than that of direct terminal purchase of gas and that the carbon emissions of direct terminal purchase of gas are smaller than those of direct terminal purchase of gas.

the system is smaller. Therefore, the two strategies, MOC and MEC, in this paper, are not conflicting objective functions, and to a certain extent, MOC and MEC are coupled to each other through the penalty factor, and the joint optimality of MOC and MEC can be achieved by selecting a penalty factor of the appropriate size.

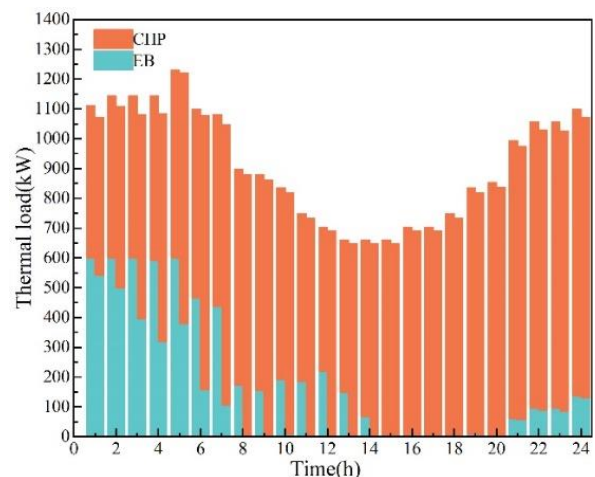


Fig. 2. Thermal load of MOC and MEC.

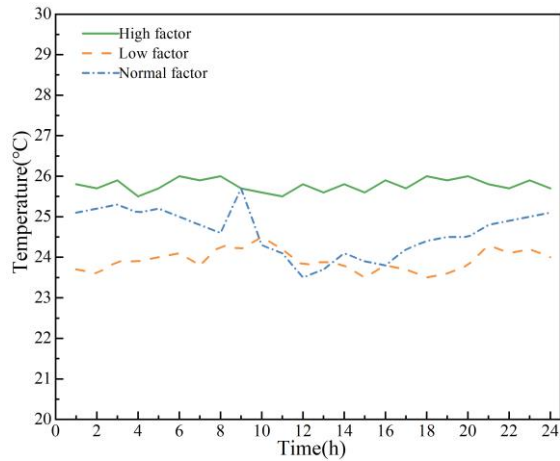


Fig. 3. Indoor temperature of various penalty factors.

TABLE III. OPTIMAL RESULTS OF MOC AND MEC.

Modes	Total carbon emissions (kg)	Carbon trading costs (¥)
MOC	15642	7890.3
MEC	13990	7056.2

TABLE IV. RESULTS OF PARETO FRONITER OF TWO CASES.

No.	Carbon emissions (kg)	Operating costs (¥)	No.	Carbon emissions (kg)	Operating costs (¥)
M	13990	45925	P	14870	42780
2	14150	44827	6	15030	42687
3	14390	44329	7	15350	42236
4	14630	43678	N	15642	42113

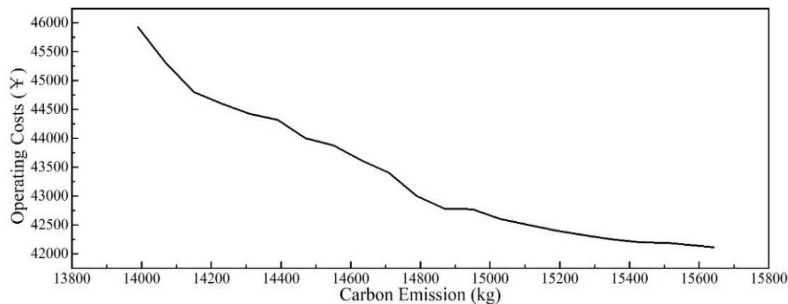


Fig. 4. Pareto frontier of two cases.

VI. CONCLUSIONS

This paper has used the GAPS0 algorithm to solve the Pareto frontier set considering system operation costs and carbon emissions.

The cases in this paper show that:

1. The system will correspondingly increase its purchases to the upper gas grid when in MEC, and the consumption of renewable energy sources will be reduced to a certain extent.
2. Electricity is more economical and gas is less carbon intensive in a small integrated energy system for end users.
3. In this paper, MOC and MEC are not conflicting objective functions, and to some extent, MOC and MEC are coupled to each other through the penalty factor, and the joint optimality of MOC and MEC can be achieved by selecting a penalty factor of the appropriate size.

CONFLICTS OF INTEREST

The authors declare that they have no conflict of interest.

REFERENCES

- [1] D. F. Dominković *et al.*, “Zero carbon energy system of South East Europe in 2050”, *Applied Energy*, vol. 184, pp. 1517–1528, 2016. DOI: 10.1016/j.apenergy.2016.03.046.
- [2] L. Sun, X. Cao, M. Alharthi, J. Zhang, F. Taghizadeh-Hesary, and M. Mohsin, “Carbon emission transfer strategies in supply chain with lag time of emission reduction technologies and low-carbon preference of consumers”, *Journal of Cleaner Production*, vol. 264, art. 121664, 2020. DOI: 10.1016/j.jclepro.2020.121664.
- [3] L. Sun, Q. Xu, J. Zhao, and Y. Ji, “Stochastic parallel optimization of an islanded microgrid under multiple source-load uncertainties”, *Journal of Renewable and Sustainable Energy*, vol. 13, no. 6, p. 065501, 2021. DOI: 10.1063/5.0065476.
- [4] J. B. Garrison and M. E. Webber, “An integrated energy storage scheme for a dispatchable solar and wind powered energy system”, *Journal of Renewable and Sustainable Energy*, vol. 3, no. 4, p. 043101, 2011. DOI: 10.1063/1.3599839.
- [5] J. Cheng, L. Mu, and Z. Liang, “Multi-objective optimization of micro-energy network considering exergy efficiency”, *Journal of Renewable and Sustainable Energy*, vol. 14, no. 3, p. 034701, 2022. DOI: 10.1063/5.0088883.
- [6] H. Yang, P. Jiang, Y. Wang, and H. Li, “A fuzzy intelligent forecasting system based on combined fuzzification strategy and improved optimization algorithm for renewable energy power generation”, *Applied Energy*, vol. 325, art. 119849, 2022. DOI: 10.1016/j.apenergy.2022.119849.
- [7] M. Geidl, G. Koeppel, P. Favre-Perrod, B. Klockl, G. Andersson, and K. Frohlich, “Energy hubs for the future”, *IEEE Power & Energy Magazine*, vol. 5, no. 1, pp. 24–30, 2007. DOI: 10.1109/MPAE.2007.264850.
- [8] E. Akbari, S. F. Mousavi Shabestari, S. Pirouzi, and M. Jadidoleslam, “Network flexibility regulation by renewable energy hubs using flexibility pricing-based energy management”, *Renewable Energy*, vol. 206, pp. 295–308, 2023. DOI: 10.1016/j.renene.2023.02.050.
- [9] S. Wang and S. Yuan, “Interval optimization for integrated electrical and natural-gas systems with power to gas considering uncertainties”,

D. Performance of Pareto Optimal Solution

Table III shows the optimal results of MOC and MEC. Therefore, this section uses the multi-objective optimisation algorithm based on the improved epsilon constraint method proposed in Section IV to solve the optimal objective N in MOC and the optimal objective M in MEC and uses the fuzzy multi-weight technology to solve the compromise solution P that gives priority to both M and N. 20 optimal solutions between M and N are selected to form the Pareto frontier, as shown in Fig. 4, and some of the solutions are listed in Table IV. The analysis of Table IV shows that the optimal solution N has a 1.6 % lower cost but 4 % higher carbon emissions compared to the compromise solution P. The optimal solution M has 6 % lower carbon emissions but 7.3 % higher costs compared to the compromise solution P.

- International Journal of Electrical Power & Energy Systems*, vol. 119, art. 105906, 2020. DOI: 10.1016/j.ijepes.2020.105906.
- [10] C. Lin, W. Wu, B. Wang, M. Shahidehpour, and B. Zhang, “Joint commitment of generation units and heat exchange stations for combined heat and power systems”, *IEEE Trans. Sustain. Energy*, vol. 11, no. 3, pp. 1118–1127, 2020. DOI: 10.1109/TSTE.2019.2917603.
- [11] T. Paterova and M. Prauzek, “Estimating Harvestable Solar Energy from Atmospheric Pressure Using Deep Learning”, *Elektronika ir Elektrotechnika*, vol. 27, no. 5, pp. 18–25, Oct. 2021. DOI: 10.5755/j02.eie.28874.
- [12] C. Wu, W. Gu, Y. Xu, P. Jiang, S. Lu, and B. Zhao, “Bi-level optimization model for integrated energy system considering the thermal comfort of heat customers”, *Applied Energy*, vol. 232, pp. 607–616, 2018. DOI: 10.1016/j.apenergy.2018.09.212.
- [13] B. Zhou *et al.*, “Optimal scheduling of biogas–solar–wind renewable portfolio for multicarrier energy supplies”, *IEEE Trans. Power Syst.*, vol. 33, no. 6, pp. 6229–6239, 2018. DOI: 10.1109/TPWRS.2018.2833496.
- [14] Y. Ding, Q. Xu, and Y. Huang, “Optimal sizing of user-side energy storage considering demand management and scheduling cycle”, *Electric Power Systems Research*, vol. 184, art. 106284, 2020. DOI: 10.1016/j.epsr.2020.106284.
- [15] S. Chen, Y. Yang, M. Qin, and Q. Xu, “Coordinated multiobjective optimization of the integrated energy distribution system considering network reconfiguration and the impact of price fluctuation in the gas market”, *International Journal of Electrical Power & Energy Systems*, vol. 138, art. 107776, 2022. DOI: 10.1016/j.ijepes.2021.107776.
- [16] Y. Wang *et al.*, “Economic and efficient multi-objective operation optimization of integrated energy system considering electro-thermal demand response”, *Energy*, vol. 205, art. 118022, 2020. DOI: 10.1016/j.energy.2020.118022.
- [17] Y. Chen, J. Wen, and S. Cheng, “Probabilistic load flow method based on Nataf transformation and Latin Hypercube Sampling”, *IEEE Trans. Sustain. Energy*, vol. 4, no. 2, pp. 294–301, 2013. DOI: 10.1109/TSTE.2012.2222680.
- [18] Q. Xu, Y. Yang, Y. Liu, and X. Wang, “An improved Latin Hypercube Sampling method to enhance numerical stability considering the correlation of input variables”, *IEEE Access*, vol. 5, pp. 15197–15205, 2017. DOI: 10.1109/ACCESS.2017.2731992.
- [19] T. Cheung, S. Schiavon, T. Parkinson, P. Li, and G. Brager, “Analysis of the accuracy on PMV – PPD model using the ASHRAE Global Thermal Comfort Database II”, *Building and Environment*, vol. 153, pp. 205–217, 2019. DOI: 10.1016/j.buildenv.2019.01.055.
- [20] Y. Chen *et al.*, “Co-optimization of passive building and active solar heating system based on the objective of minimum carbon emissions”, *Energy*, art. 127401, 2023. DOI: 10.1016/j.energy.2023.127401.
- [21] Y. Qin *et al.*, “Optimal operation of integrated energy systems subject to the coupled demand constraints of electricity and natural gas”, *CSEE Journal of Power and Energy Systems*, vol. 6, no. 2, pp. 444–457, 2020. DOI: 10.17775/CSEEJPES.2018.00640.
- [22] C. Shao, Y. Ding, J. Wang, and Y. Song, “Modeling and integration of flexible demand in heat and electricity integrated energy system”, *IEEE Trans. Sustain. Energy*, vol. 9, no. 1, pp. 361–370, 2018. DOI: 10.1109/TSTE.2017.2731786.
- [23] T. Zhang, L. Chen, and J. Wang, “Multi-objective optimization of elliptical tube fin heat exchangers based on neural networks and genetic algorithm”, *Energy*, vol. 269, art. 126729, 2023. DOI: 10.1016/j.energy.2023.126729.
- [24] Z. Xing, J. Zhu, Z. Zhang, Y. Qin, and L. Jia, “Energy consumption optimization of tramway operation based on improved PSO algorithm”, *Energy*, vol. 258, art. 124848, 2022. DOI: 10.1016/j.energy.2022.124848.
- [25] B. M. Sahoo, H. M. Pandey, and T. Amgoth, “GAPSO-H: A hybrid approach towards optimizing the cluster based routing in wireless sensor network”, *Swarm and Evolutionary Computation*, vol. 60, art. 100772, 2021. DOI: 10.1016/j.swevo.2020.100772.
- [26] R. Li, W. Wei, S. Mei, Q. Hu, and Q. Wu, “Participation of an energy hub in electricity and heat distribution markets: An MPEC approach”, *IEEE Trans. Smart Grid*, vol. 10, no. 4, pp. 3641–3653, 2019. DOI: 10.1109/TSG.2018.2833279.



This article is an open access article distributed under the terms and conditions of the Creative Commons Attribution 4.0 (CC BY 4.0) license (<http://creativecommons.org/licenses/by/4.0/>).